

Welded Joints' Heat Affected Zone's Extension Prediction by Switching Welding Parameters

Leonardo Gadelha Tumajan Costa de Melo^{a*}, Francisco Ilo Cardoso^b, Catarina Esposito Mendes^a,

Ricardo Artur Sanguinetti Ferreira^a, Paternak Souza Barros^a, Tiago Leite Rolim^a

^aDepartamento de Engenharia Mecânica - DEMEC, Universidade Federal de Pernambuco - UFPE, Rua Guilherme Pinto, 52011-210, Recife, PE, Brazil

^bDepartamento de Engenharia Mecânica - DEM, Universidade de Pernambuco, POLI/UPE, Rua Benfca, 455, Madalena, 50750410, Recife, PE, Brazil

Received: December 12, 2016; Accepted: October 18, 2017

Choosing welding parameters is an important step in welding process, directly influencing in the heat input provided to welded joints. This heat input value, along with temperature distribution in welded joints, provides, to the drafter, conditions of predicting the Heat Affected Zone (HAZ) extension, the kind of microstructure to be formed, and therefore, the effects of residual stress. Three welding parameters were switched, providing different welding conditions. Each condition was analyzed by SmartWeld 2011 software and macrography to find and compare the extension of HAZ. As for the residual stresses, calculated through Displacement of Coordinated Points (DCP) method. It is possible to choose the best parameters for the welded joint by GMAW process considering the parameters in study.

Keywords: residual stress, welding parameters, haz, displacement of coordinated points, naval sheets, gmaw

1. Introduction

In any fabrication process, some concerns must be considered. Those may be regarding finish, dimensions, chemical, electrical or most likely in welding, mechanical properties. Regarding the last ones, the properties of the weld metal itself are possible to control through the use of consumables having suitably designed alloying additions, but the heat affected zones adjacent to welds (HAZ) are often the most critical regions with regard to potential failures¹. The HAZ determines the microstructural and metallurgical changes of the weldment due to the heat generated during welding process and, usually, because of large grain microstructure, ductility and toughness of this area is poor, being the heat input the most important factor among those who affect HAZ².

Still, due to thermal influence, a material, mechanical element, or finished piece may, by the end of such process, present internal stresses. Those are named residual stresses: self-balanced stresses existing in materials in homogenous temperature conditions and with no external load³. When dealing with huge thermal variations, such stresses are introduced by the large temperature gradient due to heating and uneven cooling, and are originated mainly because of cooling contractions, contributing, as well, intense surface cooling and phase changing. In this research the used material was a heat treatable steel, therefore it is possible to affirm that the heat input and thermal gradient during welding may affect phase changing, working point by point the microstructure and the affected area's properties, resulting

in this gradient being the main responsible for the existence of residual stresses and distortions.

In the samples, welding voltage, speed and bevel angle were switched. However, in order to be able to compare and further analyze those, only one parameter was switched by each sample, while the rest of them would remain constant. For the bevel change scenario, the remaining welding parameters were constant, in a way heat input would not change. Heat input may be calculated by equation 1⁴.

$$\text{Heat Input} \left(\frac{\text{kJ}}{\text{mm}} \right) = \frac{V \times i \times 60}{v \times 1000} \times \eta \quad (1)$$

Where:

η - efficiency, process-dependent;

V - voltage (V);

I - current (A);

v - linear welding speed (mm/s).

Heat input is an important characteristic, because just like pre-heat and interpass temperature, it influences cooling rate, which affects mechanical properties and the metallurgical structure of welded and heat affected regions⁵ therefore affecting HAZ's extension and residual stresses distribution in welding.

2. Materials and Methods

2.1 Base metal

The sheets were provided by Atlântico Sul Shipyard, from Suape's Harbor - Cabo de Santo Agostinho - PE, with 1200 x 500 x 13,7 mm and ASTM A131 grade AH-36 class.

*e-mail: lgtmelo@terra.com.br

In order for the samples to be welded, they had to be prepared, being cut in 70 x 200 x 13,7 mm sizes, according to rolling direction, so the weld beads were parallel to it.

2.2 Equipment, process and welding parameters

Naval steel ASTM A-131 grade AH-36 were used to calculate residual stresses by Displacement of Coordinated Points (DCP) method and samples were extracted to evaluate ZTA's extensions. The sheets were machined as demonstrated in Figure 1, with root height of 2 mm and bevel angle of 25° or 35°.



Figure 1. Sample machining.

Weldings were performed by GMAW process with a semiautomatic MAG welding machine, as shown in Figure 2, along with a gas-cutting machine adapted to move the pistol (Figure 3), automating the operation.

The wire was AWS ER70S-6 with 1,2 mm diameter and the gas was 75% Ar and 25% CO₂. To simulate naval panel welding, side locks were inserted as a way to impose restrictions. The gas-cutting machine was aligned for the root pass and the remaining ones. The passes were in alternated directions, in order to reduce distortions. After each pass, the vitreous enamel coating was removed with a steel brush.

Four pairs of 70 x 200 mm sheets were welded, two by two, with parameters as listed in Table 1. With sample 1 as the standard, for each following sample only one parameter was switched, in a way that comparison between them was possible for each parameter. The switched parameters were bevel angle for sample 2, welding speed, for sample 3, and welding voltage, for sample 4.

2.3 Residual stresses measurement

The method that was adopted to measure residual stresses was the DCP⁶, which consists in of measuring the extension of previously mapped displacement points. For so, five holes with 2 mm depth were drilled with a 2 mm diameter (Figure 4) and their centers were mapped in X, Y.

The drilled holes distribution is as in Figure 5.



Figure 2. MAG welding semiautomatic machine.



Figure 3. Gas-cutting machine.

A Coordinated Measurement Machine (CMM) with computerized numerical control does the measuring and mapping of the drilled holes (Figure 6).

Table 1. Welding parameters.

Sample	Average Voltage (V)	Average Current (A)	Welding Speed (mm/s)	Average Input (W)	Bevel angle (°)
1	19,53	173,67	6	565,38	25
2	19,99	169,33	6	564,13	35
3	19,49	174,75	3,5	972,98	25
4	26,91	178,42	6	800,15	25



Figure 4. Sample drilled holes.



Figure 7. Sample after heat treatm.

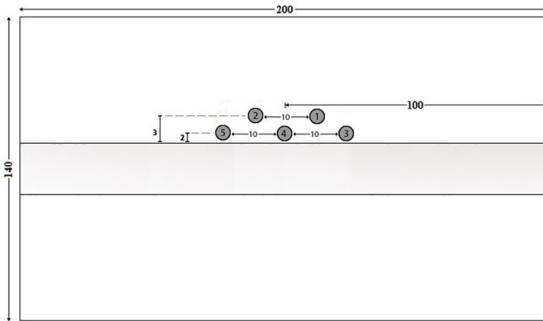


Figure 5. Holes distribution in welded samples.

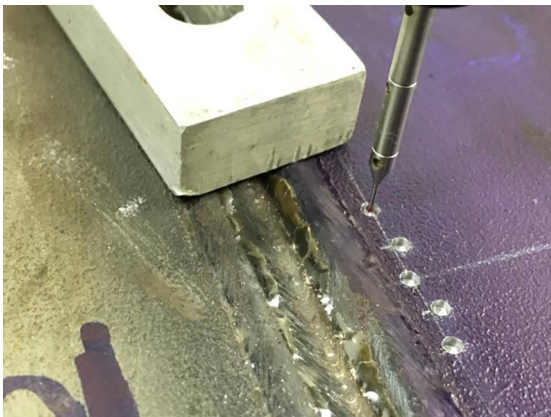


Figure 6. CMM mapping.

The next step is an annealing heat treatment (Figure 7), currently the most used method to stress relieving⁴, at 740°C in order to relieve the stresses, so it is possible to identify

the displacement of previously mapped points, due to the material's yielding. This condition happens because during the heat treatment, back stress acts reversing the barriers, contributing to the displacement in contrary direction of plastification⁷.

The mapped points were displaced due to reverse yielding and were remapped, according to the principle of coordinate measurement, which has the objective of determining dimensional parameters through coordinated points measurement over the surface of some piece and mathematically process it⁸. This makes it possible to calculate the strains through Eq. 2 in both length and crosswise direction.

$$\epsilon = \frac{\Delta L}{L_0} \tag{2}$$

Where:

ϵ : specific strain;

ΔL : variation in displacement of coordinated points (mm);

L_0 : displacement of coordinated point and sample center (mm).

With coordinated point measured before and after heat treatment, the welding strains can be found from Eq. (3) and (4)⁹:

$$\sigma_x = \frac{E}{1 - \nu^2} (\epsilon_x + \nu \epsilon_y) \tag{3}$$

$$\sigma_y = \frac{E}{1 - \nu^2} (\epsilon_y + \nu \epsilon_x) \tag{4}$$

Where:

σ_x : lengthwise residual stress – welding direction (Pa);

σ_y : crosswise residual stress – normal to welding direction (Pa);

ε_x : specific lengthwise strain;

ε_y : specific crosswise strain;

E: material's modulus of elasticity (GPa);

ν : Poisson's ratio.

Still, residual stress values σ_x and σ_y are obtained by measuring ε_x and ε_y , which are residual deformations in the points where it is desired to know the residual stresses⁹. To calculate it, modulus of elasticity of 207.000 MPa and Poisson's ratio of 0,3 were used⁷.

2.4 HAZ measurement and modeling

Since these are multilayer welds, in order to effectively measure HAZ's extension, the last pass was identified. For so, macrographies were obtained (Figure 8) from specimens obtained from each welded sample.

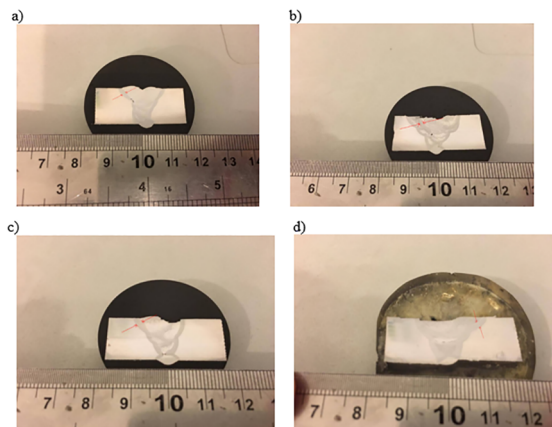


Figure 8. a) Macrography of specimen from sample 1. b) Macrography of specimen from sample 2. c) Macrography of specimen from sample 3. d) Macrography of specimen from sample 4.

The measurement was done with a dimensional measurement device from an optical microscope in the identified parts from the pictures.

To establish a comparison, some modeling of the weld bead was performed with SmartWeld 2011 software, with module ISO 2.5D. From this simulation, representations of the gradients of reached temperatures on the transverse plan of the weld bead. Then, it is only necessary to fill which temperature is desired to be displayed. It is also necessary

to choose a material from a non-editable database within the software. The ASTM A131 grade AH-36 steel is not on this list, so AISI 1018 steel was selected, for it was the closest possible match. SmartWeld does not support multilayer welding, so this was a single-pass model. Since what is under evaluation is the HAZ related to the last pass, this was not a problem. The recrystallization temperature for the steel under study is of 750°C¹⁰, so this was the adopted value to identify the isothermal that represents the beginning of HAZ.

3. Results and discussion

Residual stresses in both length and crosswise to the weld bead were calculated for each of the five points of each sample. Their modules were grouped according to the distance between the studied point and the weld bead. So points 1 and 2, which are 3 mm from the bead margin, were grouped as one average, as points 3, 4 and 5, which are 2 mm from the bead margin were grouped as another average. Both averages were listed in Table 2.

The results are consistent with the range of residual stress found in sheets of similar thickness¹¹. It is possible to observe a decrease in residual stresses when raising the bevel angle (from 25° to 35°), which demands more passes and therefore, raises the volume of deposition. Analogously, residual stresses are reduced by reducing welding speed, as well as by increasing voltage, as both scenarios imply in an increase of heat input. The heat input and layer number have great effects on residual stress distribution. With the heat input and welding layer number increasing, the residual stresses have decreased. Using multiple-layer welding and higher heat input can be useful to decrease the residual stress¹².

Table 3 lists the measurements of HAZ's extensions experimentally obtained from each specimen.

Table 3. HAZ's extensions as experimentally obtained.

Sample	HAZ's extension (mm)
1	1,80
2	1,60
3	2,10
4	2,00

Figure 9 displays the results of SmartWeld modelings.

From the models' images, HAZ's extensions were obtained, as listed in Table 4.

It is noticeable that SmarWeld is an accurate tool for uses as in the present study, and even most when taking

Table 2. Residual stresses.

Sample	$ \sigma_{1,2a} $ (MPa)	$ \sigma_{3,4,5a} $ (MPa)	$ \sigma_{y1,2a} $ (MPa)	$ \sigma_{y3,4,5a} $ (MPa)
1	184,18	202,96	232,29	252,45
2	92,08	104,34	109,56	123,68
3	18,12	14,26	25,82	19,72
4	83,49	80,51	104,16	102,83

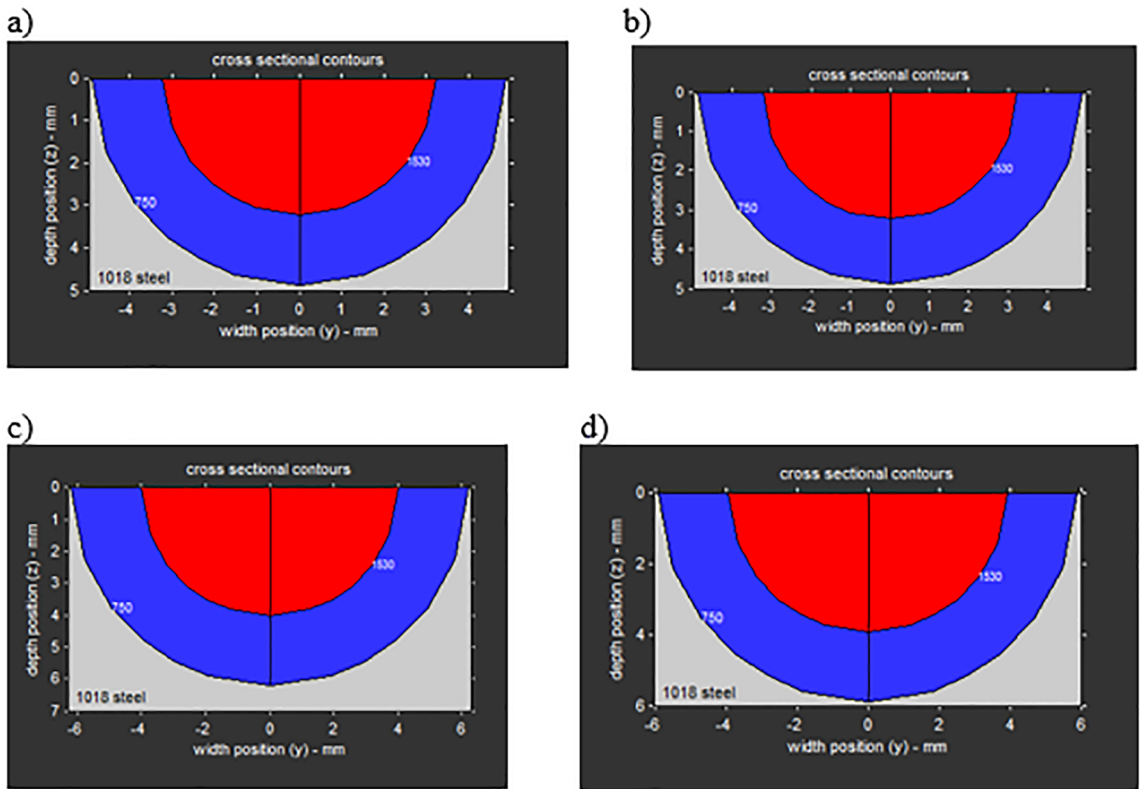


Figure 9. a) Sample 1 modeling. b) Sample 2 modeling. c) Sample 3 modeling. d) Sample 4 modeling.

Table 4. HAZ's extensions according to SmartWeld.

Sample	HAZ's extension (mm)
1	1,8
2	1,8
3	2,1
4	2,0

into account the few parameters demanded to produce such modeling. Three of the samples (no. 1, 3 and 4) presented the same HAZ extension as predicted by the software, while the only divergent sample (no 2) presents a small error, if taking into consideration the approximations and adaptations. Still, the software has no option for bevel angle configuration.

If taking solely into consideration the smaller residual stress values, smaller welding speeds should be chosen, but this would mean bigger HAZ extensions. However, if taking solely into consideration HAZ size, higher bevel angles would be the choice, which in real life would demand a greater volume of deposition, limiting this parameter, but reducing residual stresses by half.

Switching welding parameters may increase residual stress values while reducing HAZ's extension, and vice versa, so it is up to the engineer to consider every aspect when choosing them.

4. Conclusions

SmartWeld software has proved to be a reasonable tool to predict HAZ's extension for a single pass weld, presenting consistent values in comparison of the measurements of samples 1, 3 and 4. The divergence in sample 2, with bevel angle variation may be justified with the fact that the software has no option for bevel angle configuration as a parameter.

When taking into consideration bevel change from 25° to 35°, residual stresses were reduced by half, as expected.

Regarding the decrease in welding speed from 6 mm/s to 3,5 mm/s, HAZ's extension increased in 0,3 mm and residual stresses decreased between 160 and 230 MPa, showing it is possible to have a bigger HAZ, however, significantly reducing residual stresses.

For the change of welding voltage from 19,53 V to 26,91 V, HAZ's extension increased in 0,2 mm and residual stresses decreased a little over a half. Once again, showing it is possible to increase HAZ while reducing residual stresses.

5. References

- Hutchinson B, Komenda J, Rohrer GS, Beladi H. Heat affected zone microstructures and their influence on toughness in two microalloyed HSLA steels. *Acta Materialia*. 2015;97:380-391.
- Moghaddam MA, Golmezergi R, Kolahan F. Multi-variable measurements and optimization of GMAW parameters for

- API-X42 steel alloy using a hybrid BPNN-PSO approach. *Measurement*. 2016;92:279-287.
3. Macherauch E, Kloss KH. Origin, Measurements and Evaluation of Residual Stress in Science and Technology. In: Macherauch E, Hauk V, eds. *Residual Stresses in Science and Technology*. Oberusel: DGM Verlag; 1987.
 4. Modenesi PJ. *Efeitos Mecânicos do Ciclo Térmico*. Departamento de Engenharia Metalúrgica e de Materiais. Belo Horizonte: Universidade Federal de Minas Gerais - UFMG; 2001.
 5. Zinn W, Scholtes B. Residual Stress Formation Processes during Welding and Joining. In: Totten G, Howes M, Inoue T, eds. *Handbook of Residual Stress and Deformation of Steel*. Materials Park: ASM International; 2002; p. 391-396.
 6. Siqueira Filho AV, Rolim TL, Yadava YP, Cardoso FIB, Guimarães PB, Maciel TM, et al. Development of methodology for measurements of residual stresses in welded joint based on displacement of points in a coordinated table. *Materials Research*. 2013;16(2):322-326.
 7. Mendes CE, Ferreira RAS, Melo LGTC, Barros PS, Gonçalves IL, Rolim TL, et al. Influence of Rolling Direction in Calculation of Residual Stress by Using DCP Method in Naval Welded Sheets. In: *23rd ABCM International Congress of Mechanical Engineering (COBEM 2015)*; 2015 Dec 6-11; Rio de Janeiro, RJ, Brazil.
 8. Rolim TL. *Sistemática indicadora de método para calibração de máquinas de medição por coordenadas*. [Tese]. João Pessoa: Universidade Federal da Paraíba; 2003.
 9. Okumura T, Tanigusgi C. *Engenharia de soldagem e aplicações*. Rio de Janeiro: Livros Técnicos e Científicos; 1982.
 10. Gonçalves IL. *Influência da Temperatura no Tratamento de Alívios de Tensões em uma Junta Soldada Baseado no Método DPC*. [Dissertation]. Recife: Universidade Federal de Pernambuco; 2015.
 11. Kim TJ, Jang BS, Kang SW. Welding deformation analysis based on improved equivalent strain method considering the effect of temperature gradients. *International Journal of Naval Architecture and Ocean Engineering*. 2015;7(1):157-173.
 12. Jiang WC, Wang BY, Gong JM, Tu ST. Finite element analysis of the effect of welding heat input and layer number on residual stress in repair welds for a stainless steel clad plate. *Materials & Design*. 2011;32(5):2851-2857.